Proceedings of the 8th International Conference on Civil Engineering for Sustainable Development (ICCESD 2026), 5~7 February 2026, KUET, Khulna, Bangladesh

ANISOTROPIC DAMPING BEHAVIOR IN PARTIALLY BONDED BASE ISOLATORS MADE FROM SQUARE SHAPED SCRAP TIRE RUBBER

Md. Mistak Hossain*[1]

[1]*Graduate Student, North South University, Bangladesh, e-mail: u1801009@student.cuet.ac.bd, mistak.hossain.253@northsouth.edu*

***Corresponding Author**

ABSTRACT

The damping impact related to the seismic performance of 100mm×100mm×24mm shaped STRP isolators with different bonding levels is the main topic of this paper. Base of a scrap tire rubber pad for remote or rural locations or seismically active sites, isolators constructed from recycled tires offer an economical and environmentally responsible substitute. Using Marc Mentat software for this FEA analysis, the isolators are tested at bi-directional loading angles and bonding levels (0%, 25%, 50%, 75%, and 100%) in order to assess their energy absorption. The findings show that STRP-50 has most energy absorption capacity among all of them. Initially it drops but when come to 50% bonded it rises and found lowest at fully bonded. Though all of from this shaped isolator; damping results are shown less than other square shaped isolators. The different effective damping of partially bonded models under different loading orientations and displacements illustrates the benefits of partial bonding. These results suggest that partially bonded STRP isolators are most beneficial for buildings that need more effective dampening.

Keywords: *Anisotropic, STRP, Seismic performance, Damping, Base Isolator.*

1. INTRODUCTION

Rural buildings in earthquake-prone developing nations are susceptible to destruction because of inadequate seismic design and subpar construction. In these nations, seismic design requirements are often disregarded to reduce building costs, thereby lowering a structure's seismic performance. Because of this, even a minor earthquake can have catastrophic consequences, resulting in significant loss of life and property. Large sections, steel-reinforced elastomeric isolators (SREI), and high-strength concrete are typically utilized to increase a building's resistance to seismic forces (Kalfas et al., 2020). Because of its excellent aseismic performance, SREI base isolation is widely used. Nevertheless, the structures become more expensive when these methods are used.

Promoting locally made, inexpensive base isolators is one of the best ways to address the cost issue. Several researchers have proposed the scrap tire rubber pad (STRP) isolators, which are made from car tires. Because waste tires are inexpensive and the STRP isolator requires only construction costs, it is considered a sustainable and economical base-isolation solution, particularly in developing nations (Zisan & Igarashi, 2021), (Zisan et al., 2023), (Zisan & Igarashi, 2022), (Mishra, 2012). The evaluation of unbonded STRP isolators using experimental investigations and the finite element approach was the primary focus of earlier STRP isolator research (Mishra, 2012), (Zisan & Igarashi, 2021), (Zisan et al., 2023). The lateral load was thought to be transferred by friction in an unbonded STRP isolator. An STPR isolator without mechanical bonding to structural components was shown to exhibit favourable outcomes, suggesting the possibility of effectively using sustainable technology (Zisan & Igarashi, 2021), (Zisan & Igarashi, 2022). In lateral loading situations, a STRP isolator without mechanical bonding shows distinct rollover deformation. This unbounded condition reduces the likelihood of tensile cracks by preventing high tensile loads at the base isolator (Zisan & Igarashi, 2021), (Mishra, 2012). Zisan and Igarashi investigated the performance of an unbonded STRP isolator under various loading directions (Zisan & Igarashi, 2022). However, because STRP isolators may slip or topple due to unusual eccentricity, it is impractical to mount a structure on a base isolator without mechanical fastening (Zisan et al., 2023) (Engelen, 2019). Partial bonding of the STRP isolator with the structural element would be a better way to reduce the risk of slippage or isolator overturning (Engelen et al., 2014). Finding the damping behaviour by using lateral performance of a partially bonded square-shaped STRP isolator under various orientations, such as 0°, 15°, 30°, 45°, 60° and 75° of bi-directional component cyclic loading on 100 mm x 100 mm x 24 mm model, is the goal of this work.

2. SCRAP TIRE RUBBER PAD BASE ISOLAOTR

The construction of a Scrap Tire Rubber Pad (STRP) layer is explained by (Mishra, 2012). Bridgestone 385/65R22.5 tires were used to make the STRP isolator employed in this investigation. It is made up of five 12 mm thick layers of reinforcement. These reinforcing layers are positioned at a ±70° angle to the steel carcass, as shown in Fig. 1(b). The construction process, which comprises stacking the layers, attaching them, and adding steel and rubber reinforcing cords, is shown in Fig. 1(a). These cables are arranged like steel plates in conventional laminated elastomeric bearings to provide vertical rigidity and stop lateral bulging. Table 1 lists the material and geometric properties of steel chords. Table 1 lists the features of the steel wires from the Bridgestone tires. In this study, a square-shaped STRP isolator with dimensions of 100 mm × 100 mm × 24 mm is employed. According to Table 2, isolators with bonding percentages of 0%, 25%, 50%, 75%, and 100% with structural elements are called STRP-0, STRP-25, STRP-50, STRP-75, and STRP-100, respectively. The specimens used in this investigation are described in detail in Table 2. Rubber modelling uses the Mooney-Rivlin model to accurately describe rubber's nonlinear elastic behaviour. Mishra used uniaxial testing to estimate the hyper-elastic material constants for the three-term Mooney-Rivlin energy function (Mishra, 2012). Table 3 lists the material constants used for rubber.

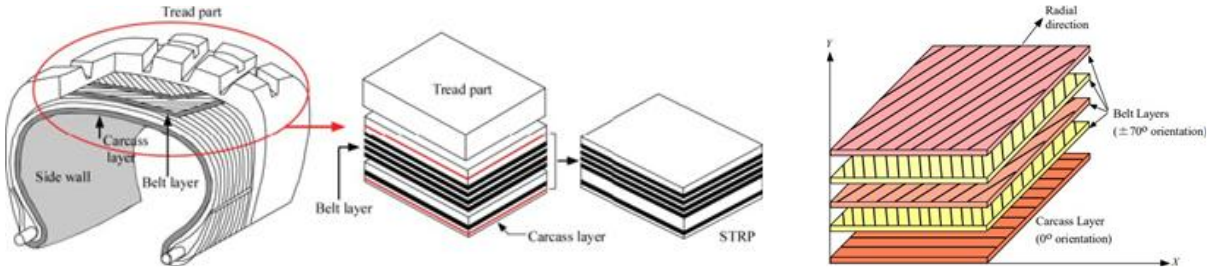

(a) (b)

Figure 1: STRP isolator: (a) Fabrication of STRP specimen; (b) Arrangement of steel reinforcing cords (Mishra, 2012)

Table 1: Properties of steel reinforcing cords (Zisan & Igarashi, 2021) (Hossain et al., 2024)

Layer	Poisson's ratio,υ	No. of filament	Filament dia (mm)	Steel cord area (mm^2)	Angle	Equivalent Thickness *tf* (mm)	Yield strength (GPa)	Modulus of elasticity *E*, (GPa)
Carcass	0.3	5	0.2	0.44	0°	0.40	2800	200
Belt	0.3	14	0.4	0.63	±70°	0.40	2800	200

Table 2: Geometric properties of STRP isolators

Model	Percentage (%) bond	Size (h×w×t) (mm)	Bonding area (mm)
STRP-0	0	100 × 100 × 24	0 × 0
STRP-25	25		50 × 50
STRP-50	50		71 × 71
STRP-75	75		87 × 87
STRP-100	100		100 × 100

Table 3: Mooney-Rivlin constants

C_{10}	C_{01}	C_{11}
0.40	1.22315	0.18759

3. FINITE ELEMENT (FE) ANALYSIS

STRP isolators are modelled and analysed using finite elements with the Marc-Mentat program (Marc, 2018). Rubber is simulated as an isoperimetric element because it can accurately model complicated, nonlinear deformations under high-strain situations. Rubber serves as the host material for the steel chord in the belt and the layers of the carcass. To approximate partial bonding of the STRP with the top and bottom surfaces of the isolator, two distinct components are modelled, as shown in Fig. 2(a)–2(c). This graphic displays STRP models with varying bonding-area percentages. The top surface of the isolator can move in both vertical and horizontal directions, but the bottom surface, which represents the building and foundation, is stationary in all dimensions. Figures 3(a) and 3(b) show the finite element models of steel chords and STRP isolators with fine mesh, respectively. The top surface of each model is subjected to a static axial load of 5 MPa. Figure 3(c) shows a full finite element model with all boundary conditions. Six cycles, or shear displacements of 25%, 50%, 100%, 150%, 200%, and 250%, make up the cyclic lateral displacement, as shown in Fig. 3(d). This lateral displacement is administered in two orthogonal directions of the isolator after being divided into two components according to the displacement's orientation. These components are oriented at 0° to 75° at the 15° interval with respect to the orthogonal direction. While the contact between the

unbonded portion of the isolator and building components is supposed to be a touched connection, the contact between rubber elements and bonded portions, as well as between building components and bonded parts, is assumed to be glued. For touch connections, a friction coefficient of 0.8 is taken into consideration (Zisan & Igarashi, 2021). Finding the effective damping of these models are the main priority for this work.

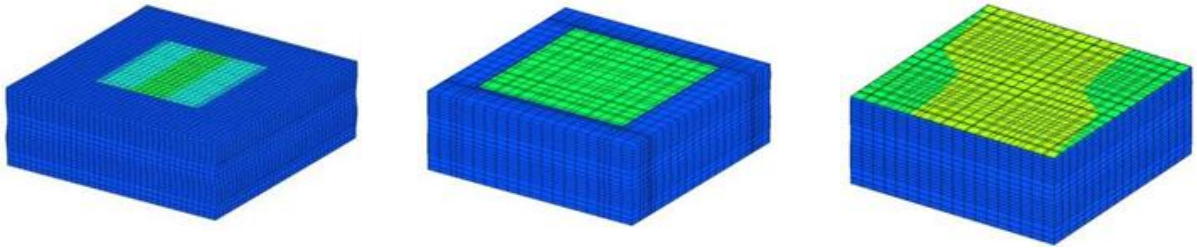

(a) 25% (b) 50% (c) 100%

Figure 2: Bonded portion of STRP: (a) STRP-0; (b) STRP-50; (c) STRP-100

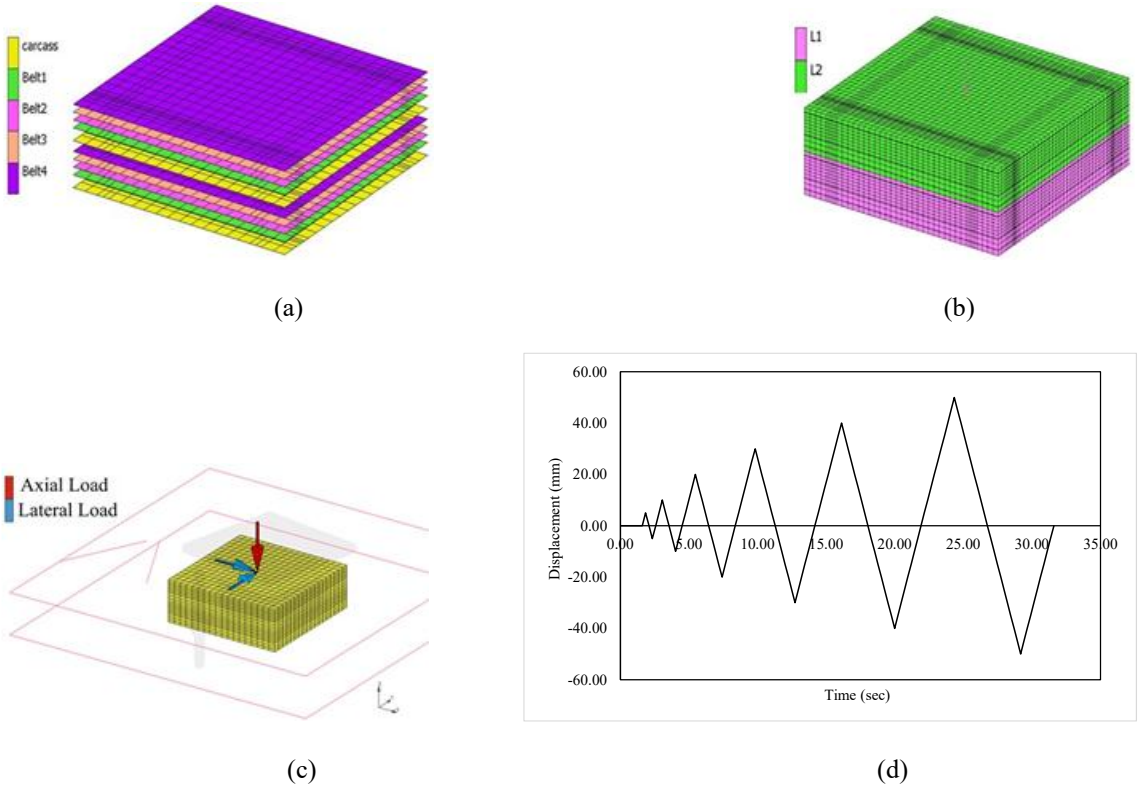

(a) (b)

(c) (d)

Figure 3: FE modelling of STRP : (a) Position of the embedded rebar components; (b) FE model mesh generation; (c) boundary conditions; (d) Lateral loading pattern

4. FINITE ELEMENT (FE) MODEL VALIDATION

The FE model STRP-0 is validated by comparing the effective damping of the isolator with the Ref. Model, as established by (Hossain, et. al., 2024). We compare the damping values of the 100mm × 100mm × 24mm model with those of the 72mm × 72mm × 24mm versions. A larger rubber pad exhibits superior shock absorption capabilities compared to a smaller, shaped cushion. Have compared fully bonded STRP base isolators measuring 72mm in square shape under loading directions of 0° and 60°. In the figure, both isolators have decreased with a percentage of shear

displacement. Although they exhibit nearly identical patterns and their slopes are closely aligned, the reference model graph has a negative slope, whereas the produced model have been demonstrated a negative slope too. The strong graph pattern connection between the Reference model and the Performed model suggests that the developed finite element model is suitable for further parametric investigation.

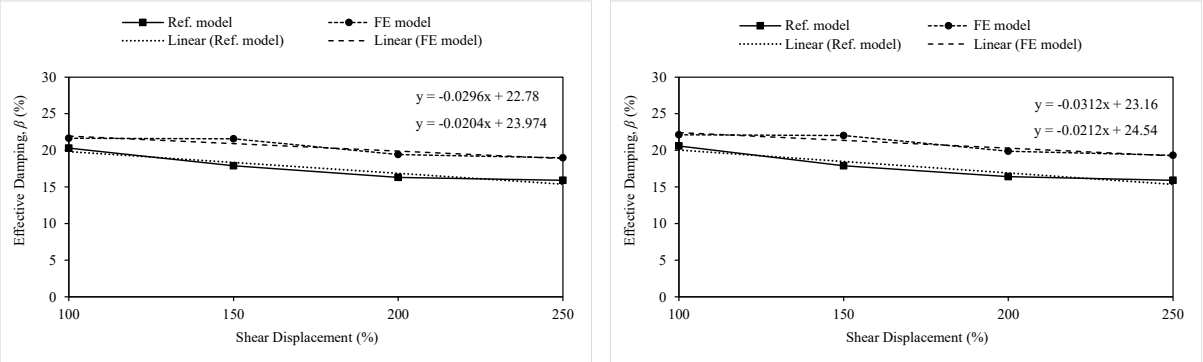

(a) (b)

Figure 4: Validation of the FE model against the reference model

5. RESULTS AND DISCUSSIONS

5.1 Relationship between Force and Displacement

The cycle lateral load response of STRP isolators subjected to cyclic shear displacements ranging from 25% to 250% under different bond percentages and loading conditions are shown in Figures 5 and 6. Table 4 provides a summary of the chosen loading situations.

Table 4: Loading conditions adopted for cyclic lateral load analysis of STRP isolators

Bond Percentage	Loading Angle	Loading Direction	Shear Displacement
0%	15º	X-direction	25%-250%
50%	30º	Y-direction	25%-250%
75%	45º	X-direction	25%-250%
100%	45º	Y-direction	25%-250%

Only four curves are described here because each loading direction has demonstrated the same pattern for its own bonded area. Additionally, the 25% bonded portion has demonstrated almost the same curve as the 50% bonded region for various loading directions. The results demonstrates that under static stress conditions, all isolators display stability, with no slippage detected in the entirely unbonded STRP isolator. The effective damping obtained from the areas of these hysteresis curves is elaborated in the following section.

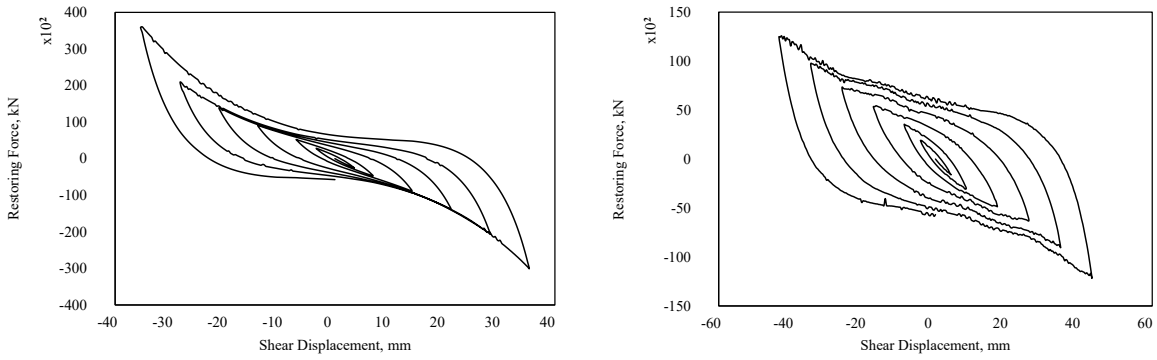

Figure 5: Un-Bonded X Axis hysteresis curve at 15º Loading; (b) 50% Bonded Y Axis hysteresis curve at 30º Loading

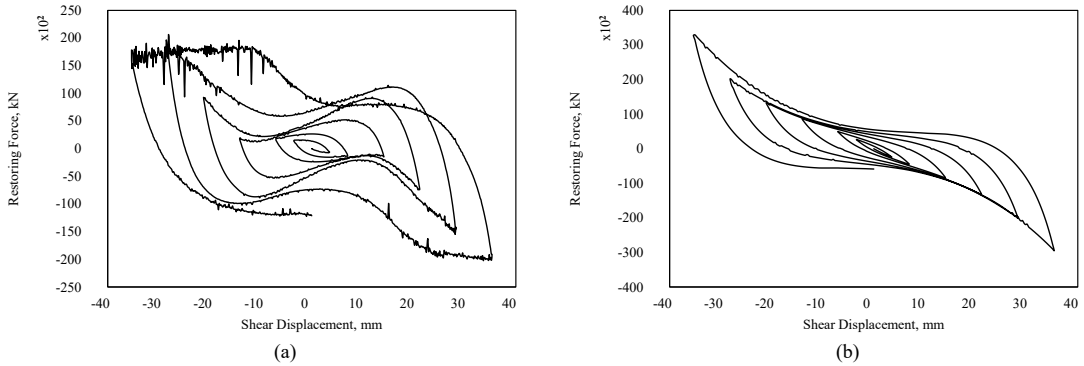

Figure 6: (a) 75% Bonded X Axis hysteresis curve; (b) 100% Bonded Y Axis hysteresis curve at 45º Loading

5.2 Effective Damping

The effective damping (β) of the STRP isolator is computed using the following equation (ASCE/SEI 7-10, 2010):

$$\beta = \frac{2}{\pi}\left[\frac{E_{loop}}{K_h\,(u^{+}-u^{-})^2}\right] \qquad (1)$$

In this application, K_h denotes the lateral stiffness on the hysteresis curve, corresponding to the greatest positive displacement, u+, and the maximum negative displacement, u^-, E_{loop} is the area of curve. The effective damping values of STRP isolators are displayed in Tables 5 through 10. Figures 7 and 8 indicate the correlation between the maximum and minimum damping ratios and the loading direction. At a 0° orientation, STRP-100 demonstrates the minimal damping value, indicating limited shock absorption capability. STRP-50 exhibits optimal effective damping at a loading angle of 45°. As the bonding area increases, the effective damping value gradually decreases, reaching its peak at STRP-50 before further declining with a larger bonded fraction. Moreover, effective damping escalated with an initial increase in lateral displacement, peaking at 250% displacement; however, at STRP-0 and STRP-25, it initially rose to 150% shear displacement before thereafter declining. Because of variations in the elastomeric system's deformation-mode interaction, strain uniformity, and load transfer efficiency, the effective damping was shown to differ with bonding % and loading angle. While increased bonding promoted uniform shear deformation and improved effective damping through an increased hysteresis loop area, incomplete interfacial bonding allowed localized slip and non-uniform deformation at low bonding percentages, limiting hysteretic energy dissipation. On the other hand, excessive bonding introduced over-constraint, increased stiffness dominance, and

suppressed internal micro-sliding and viscoelastic rearrangement, causing the effective damping to plateau or slightly decrease. The relative contributions of shear and normal stress components determined the loading angle's impact. Shear-dominated deformation at low angles and stiffness-controlled axial deformation at high angles limited energy dissipation, whereas intermediate angles allowed for combined shear-normal deformation and the simultaneous activation of several dissipation mechanisms. As a result, STRP-50 showed the best effective damping at a loading angle of 45°, where a balanced contribution of normal and shear stresses, along with adequate but not excessive bonding, maximized internal friction, interfacial micro-slip, and viscoelastic deformation, resulting in peak hysteretic response.

Table 5: Effective Damping for STRP models at 0 degree

Shear Displacement (%)	STRP-0 β (%)	STRP-25 β (%)	STRP-50 β (%)	STRP-75 β (%)	STRP-100 β (%)
25	12.34	12.23	16.73	20.13	12.03
50	18.08	17.88	26.06	19.76	18.04
100	23.43	23.36	28.98	26.44	21.66
150	23.95	23.75	31.95	29.51	21.56
200	22.43	23.16	33.14	31.62	19.44
250	23.65	23.59	34.22	31.43	18.97

Table 6: Effective Damping for STRP models at 15 degree

Shear Displacement (%)	STRP-0 β (%)	STRP-25 β (%)	STRP-50 β (%)	STRP-75 β (%)	STRP-100 β (%)
25	12.43	12.31	16.98	20.22	12.14
50	18.17	18.02	26.14	20.21	18.16
100	23.52	23.47	29.31	27.78	21.72
150	24.02	23.85	32.79	29.72	21.74
200	22.56	23.22	33.85	31.79	19.52
250	23.71	23.66	34.76	31.54	19.03

Table 7: Effective Damping for STRP models at 30 degree

Shear Displacement (%)	STRP-0 β (%)	STRP-25 β (%)	STRP-50 β (%)	STRP-75 β (%)	STRP-100 β (%)
25	16.12	15.84	17.25	20.71	12.25
50	24.46	26.43	26.64	20.35	18.3
100	26.77	29.19	29.44	27.94	21.86
150	28.11	31.64	32.93	29.88	21.85
200	29.47	33.56	33.94	31.94	19.66
250	28.22	34.01	34.88	31.65	19.15

Table 8: Effective Damping for STRP models at 45 degree

Shear Displacement (%)	STRP-0 β (%)	STRP-25 β (%)	STRP-50 β (%)	STRP-75 β (%)	STRP-100 β (%)
25	16.33	16.17	17.79	20.81	12.67
50	26.97	26.84	27.21	26.96	18.75
100	30.03	29.55	30.12	29.31	22.47
150	32.22	32.13	33.3	32.33	22.19
200	34.12	34.01	34.55	33.89	20.53
250	33.98	34.33	35.67	32.25	19.36

Table 9: Effective Damping for STRP models at 60 degree

Shear Displacement (%)	STRP-0 β (%)	STRP-25 β (%)	STRP-50 β (%)	STRP-75 β (%)	STRP-100 β (%)
25	16.22	16.05	17.44	20.98	12.45
50	26.85	26.61	26.85	20.54	18.42
100	29.88	29.4	29.64	28.11	22.13
150	32.11	31.94	33.13	30.17	22.01
200	33.97	33.75	34.13	32.17	19.87
250	34.31	34.22	35.44	31.87	19.31

Table 10: Effective Damping for STRP models at 60 degree

Shear Displacement (%)	STRP-0 β (%)	STRP-25 β (%)	STRP-50 β (%)	STRP-75 β (%)	STRP-100 β (%)
25	16.12	15.96	17.32	20.78	12.33
50	26.66	26.51	26.73	20.46	18.36
100	29.84	29.28	29.56	28.01	22.06
150	31.84	31.78	33.05	30.06	21.94
200	33.88	33.67	34.03	32.12	19.75
250	34.22	34.13	35.32	31.79	19.23

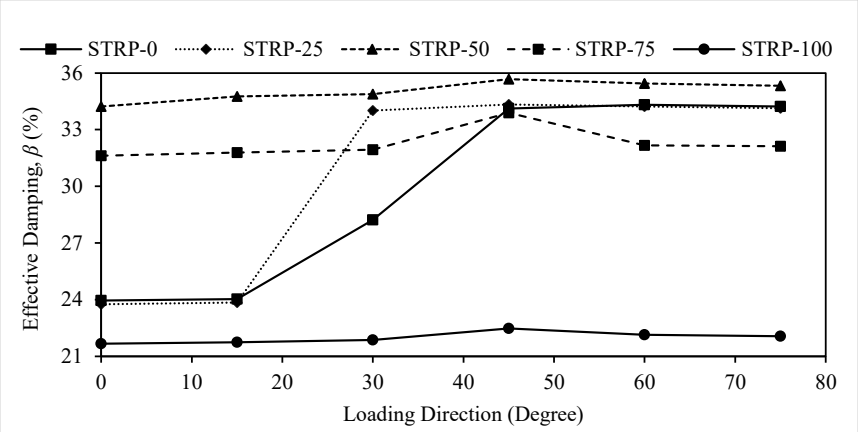

Figure 7: Highest Effective Damping for STRP

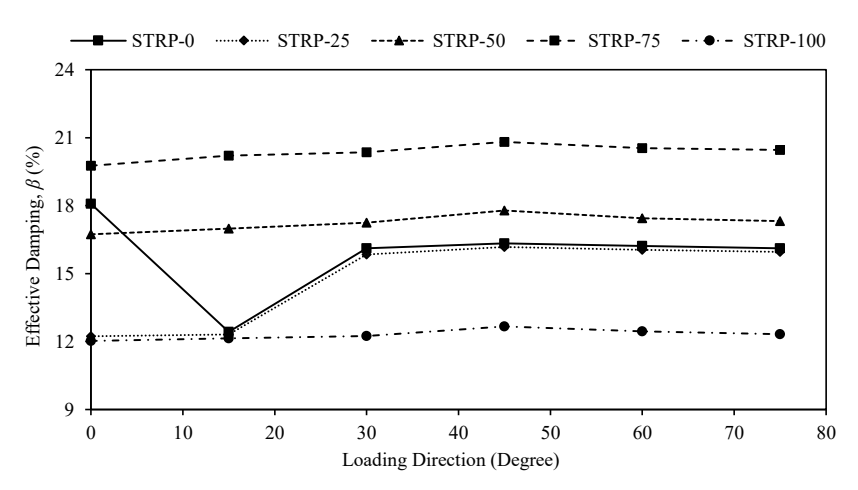

Figure 8: Lowest Effective Damping for STRP

6. CONCLUSIONS

This study investigates the lateral load performance of STRP isolators with varying bonding areas between the isolator and structural levels subjected to cyclic bi-directional lateral stress. Only square-shaped isolators subjected to cyclic loads at orientations from 0° to 75° in 15° increments are assessed. The primary conclusions are as follows:

- STRP-50 (partially bonded) exhibits enhanced efficacy in seismic isolation for this criterion; nevertheless, its efficiency declines as the quantity of bonded connections between the isolator and structural components rises.
- Furthermore, STRP-0 and STRP-25 exhibit reduced damping compared to STRP-50. Initially, from STRP-0 to STRP-25, the damping value diminishes with the increase of the bonded portion; however, at STRP-50, it reaches its peak before subsequently declining at STRP-75, with STRP-100 exhibiting the lowest value. The STRP-100 (fully bonded) isolator demonstrates the least seismic isolation effectiveness owing to its maximum lateral rigidity.
- The highest effective damping observed was 35.67% in the 50% bonded portion under 45-degree loading at 250% shear displacement, while the lowest, measured at STRP-100, was 12.03% under 0-degree loading at 25% displacement.
- Additionally, with a 25% displacement, the STRP-75 exhibits the best effective damping. These findings provide guidance for the selection of STRP isolators in structural applications, depending on the necessary damping and flexibility.

DECLARATION OF USE OF AI

The author attests that QuillBot, an AI-based technology, was exclusively used for linguistic refinement, which includes rewording sentences and fixing syntax to improve the manuscript's overall readability. The research design, data processing, analysis of the results, and creation of scientific arguments were all done without the use of the instrument. The authors alone developed the conclusions and intellectual content of this work.

REFERENCES

Marc-Mentat, MSC. (2018). Theory and user information, Vol. A, Santa Ana, CA: MSC Software Corporation.

Engelen, N. C. V. (2019). “Fiber-reinforced elastomeric isolators: A review,. *Soil Dynamics and Earthquake Engineering*, Volume 125, 105621.

Mishra, H. K. (2012). *“Experimental and Analytical Studies on Scrap Tire Rubber Pads for Application to Seismic Isolation of Structures”.* Kyoto: Kyoto University, Japan.

Hossain, M. M., Zisan, M. B., Maher, S. K., & Abdullah, N. (2024). “Effect of Loading Directionality on Seismic Behavior of Partially Bonded Square-Shaped Scrap Tire Rubber Pad Isolator,”. *Proceedings of the 7th International Conference on Advances in Civil Engineering (ICACE2024)* (pp. 2471–2478), Chattogram.

Kalfas, K. N., Mitoulis, S. A., & Konstantinidis, D. (2020). “Influence of Steel Reinforcement on the Performance of Elastomeric Bearings,. *Journal of Structural Engineering*, Volume 146, Issue 10.

Engelen, N. C. V., Osgooei, P. M., Tait, M. J., & Konstantinidis, D. (2014). “Partially bonded fiber-reinforced elastomeric isolators (PB-FREIs),". *Structural Control and Health Monitoring*, 417–432.

Zisan, M.B., & Igarashi, A. (2021). “Lateral load performance and seismic demand of unbonded scrap tire rubber pad base isolators,”. *Earthquake Engineering and Engineering Vibration*, 20(3), p. 803–821.

Zisan, M.B., & Igarashi, A. (2021). “Evaluation of unbonded Strip-STRP bearing based on current design guidelines,”. *IABSE Congress – Resilient technologies for sustainable infrastructure*, 1247-1256.

Zisan, M.B., Hasan, M.A., & Haque, M.N. (2023). "Performance assessment of buildings seismically isolated with scrap tire rubber pad isolators,". *Asian Journal of Civil Engineering*, 287–307.

Zisan, M.B., & Igarashi, A. (2022). "Effect of Loading Directionality on the Horizontal Stiffness of Unbonded Scrap Tire Rubber Pad Isolator.". *6th International Conference on Advances in Civil Engineering. ICACE 2022.* Chattogram: ICACE 2022.